

**COMMUNICATION**

# Replacing voltage sensor arginines with citrulline provides mechanistic insight into charge versus shape

Daniel T. Infield<sup>1,2</sup>, Elizabeth E.L. Lee<sup>3</sup> , Jason D. Galpin<sup>1,2</sup>, Grace D. Galles<sup>1,2</sup>, Francisco Bezanilla<sup>3,4</sup> , and Christopher A. Ahern<sup>1,2</sup> 

**Voltage-dependent activation of voltage-gated cation channels results from the outward movement of arginine-bearing helices within proteinaceous voltage sensors. The voltage-sensing residues in potassium channels have been extensively characterized, but current functional approaches do not allow a distinction between the electrostatic and steric contributions of the arginine side chain. Here we use chemical misacylation and in vivo nonsense suppression to encode citrulline, a neutral and nearly isosteric analogue of arginine, into the voltage sensor of the *Shaker* potassium channel. We functionally characterize the engineered channels and compare them with those bearing conventional mutations at the same positions. We observe effects on both voltage sensitivity and gating kinetics, enabling dissection of the roles of residue structure versus positive charge in channel function. In some positions, substitution with citrulline causes mild effects on channel activation compared with natural mutations. In contrast, substitution of the fourth S4 arginine with citrulline causes substantial changes in the conductance–voltage relationship and the kinetics of the channel, which suggests that a positive charge is required at this position for efficient voltage sensor deactivation and channel closure. The encoding of citrulline is expected to enable enhanced precision for the study of arginine residues located in crowded transmembrane environments in other membrane proteins. In addition, the method may facilitate the study of citrullination in vivo.**

## Introduction

Voltage-gated potassium channels are composed of four identical subunits, each containing a voltage-sensing domain (VSD; helices S1–S4) and a pore domain (S5 and S6) (Yellen, 1998; Jan and Jan, 2012). The VSD S4 helix contains highly conserved basic amino acids at every third position (Fig. 1). Changes in transmembrane potential act directly on a subset of these residues (arginine residues R1–R4), causing them to move through the electric field (Yang and Horn, 1995; Aggarwal and MacKinnon, 1996; Seoh et al., 1996; Yang et al., 1996). The movement of S4 is in turn mechanically coupled to pore domain opening and closing (Bezanilla and Perozo, 2003). This mechanism of activation is generally conserved with sodium and calcium channels, two other channel types that, along with potassium channels, act to coordinate the action potential in excitable cells (Bezanilla, 2000). In addition to their role in activation, voltage-sensing arginine residues play important roles in the mechanism of modulation of voltage-gated channel function by small molecule inhibitors (Ahuja et al., 2015) and by therapeutic lipids (Ottooson et al., 2014). Finally, voltage-sensing arginine residues of voltage-gated channels are commonly found mutated in disease (Cannon, 2010). As a result, this region is a subject of intense interest.

Early studies of arginine residues in the voltage sensor of the *Shaker* potassium channel demonstrated that mutation of different positions nonequivalently affects channel activation (Papazian et al., 1991). In some positions, mutation of arginine to the charge-sparing lysine caused less-pronounced effects compared with that of charge-eliminating mutations, suggesting an explicit electrostatic role of these arginine residues in gating (Papazian et al., 1991). Indeed, crystal structures of activated (depolarized) potassium channels show these arginine residues paired with highly conserved negatively charged residues from S1 and S2 (Long et al., 2005, 2007). Contemporary structural models of potassium channel activation propose that the voltage-sensing arginine residues sequentially interact with these negatively charged residues as the S4 helix moves from an inward to outward position (Henrion et al., 2012; Jensen et al., 2012; Delemotte et al., 2015). In so doing, the helix must also pass through a tight “plug” wherein the gating charges interact with conserved hydrophobic amino acids from nearby helices (Yang et al., 1996; Starace and Bezanilla, 2001; Tao et al., 2010; Lacroix and Bezanilla, 2011; Fig. 1). The lack of an atomic-scale structure of a deactivated or intermediate state of a voltage-gated channel has limited the visualization of the movements associated with

<sup>1</sup>Department of Molecular Physiology and Biophysics, The University of Iowa, Iowa City, IA; <sup>2</sup>Iowa Neuroscience Institute, The University of Iowa, Iowa City, IA;

<sup>3</sup>Department of Biochemistry and Molecular Biology, The University of Chicago, Chicago, IL; <sup>4</sup>Institute for Biophysical Dynamics, The University of Chicago, Chicago, IL.

Correspondence to Christopher A. Ahern: [christopher-ahern@uiowa.edu](mailto:christopher-ahern@uiowa.edu).

© 2018 Infield et al. This article is distributed under the terms of an Attribution–Noncommercial–Share Alike–No Mirror Sites license for the first six months after the publication date (see <http://www.rupress.org/terms/>). After six months it is available under a Creative Commons License (Attribution–Noncommercial–Share Alike 4.0 International license, as described at <https://creativecommons.org/licenses/by-nc-sa/4.0/>).

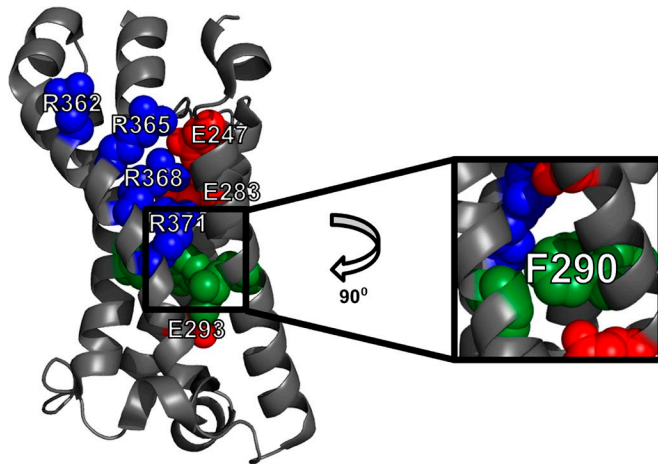


**Figure 1. Crystal structure of the *Kv* 1.2/2.1 chimera suggests electrostatic accommodation of gating charges within the voltage sensing domain.** Labels correspond to the residues at homologous positions in *Shaker*. Voltage-sensing arginine residues are shown in blue, conserved glutamate residues are shown in red, and hydrophobic residues, including the conserved phenylalanine in the hydrophobic plug (F290 in *Shaker*), are shown in green.

voltage-sensor activation and deactivation. More fundamentally, it is not well understood whether or how the energetic contributions originating purely from electrostatic components affect the stability of specific functional states.

To quantify electrostatic effects explicitly, one would like to selectively neutralize the charge of arginine while leaving other critical features of the side chain (such as shape and polarity) unchanged. Such an approach is uniquely required to the study of the distal guanidinium groups of the S4 charges in voltage sensors, because their relationship with the surrounding domain is proposed to be akin to a permeant ion through an ion channel selectivity filter (Starace et al., 1997; Tombola et al., 2005; Sokolov et al., 2007). Neither conventional mutagenesis nor substituted cysteine modification allow for the alteration of charge without significant, concomitant changes in molecular shape. The amino acid citrulline, an uncharged arginine analogue, may better serve this purpose. This naturally occurring metabolite is present in the cytoplasm of diverse cell types; it serves as an anabolic precursor to arginine in the urea cycle (Gamble and Lehninger, 1973) and a by-product of nitric oxide synthesis from arginine (Nakata et al., 1997). This amino acid is not directly encoded because it lacks an explicit synthetase, but it is found within proteins as a result of the posttranslational deimination of arginine residues (György et al., 2006). There is evidence from prior *in vitro* translation studies that citrulline is tolerated by the prokaryotic ribosome and stable in a cellular milieu (Judice et al., 1993; Choudhury et al., 2007). Additionally, citrulline has been substituted for arginine in the active sites of some enzymes by using chemical semisynthesis (Kienhöfer et al., 2003; Burschowsky et al., 2014). Critically, citrulline retains the overall architecture of the distal guanidinium group of arginine (Fig. 2 A).

Here we have used the nonsense suppression method in conjunction with chemical aminoacylation to encode citrulline into the voltage sensor of the *Shaker* potassium channel expressed in the eukaryotic *Xenopus laevis* oocyte. The observed functional

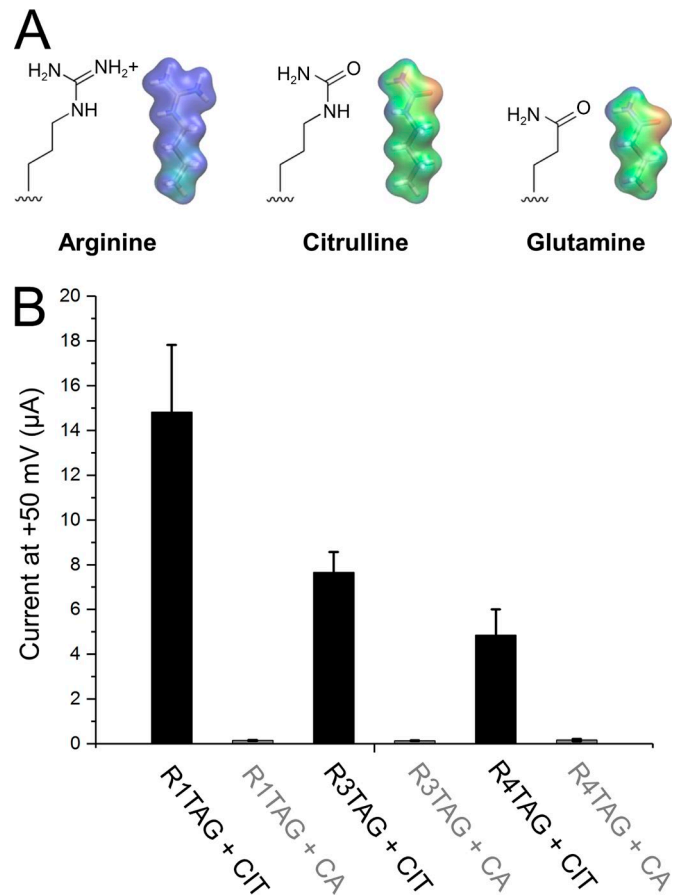


**Figure 2. Encoding of citrulline into *Shaker*.** (A) Structural and electrostatic representations of the side chains of arginine, citrulline, and glutamine. (B) Currents generated from co-injection of cRNA encoding R1TAG, R3TAG, and R4TAG with CIT-tRNA compared with those injected with cRNA and full-length (pCA-ligated) tRNA in parallel. Lack of expressed current in the pCA condition for a given position is consistent with faithful encoding of citrulline. Error bars indicate SEM.

effects at three different sites together suggest that citrulline substitution at these positions minimizes the penalties to activation caused by steric losses and clashes within the tight molecular pathway of the voltage sensor gating pore. In an experimental context wherein steric changes are minimized, the positive charge at R4 emerges as playing an outsized role in the deactivation of the channel.

## Materials and methods

### Synthesis of citrulline-phosphodexoxycytosine phosphoadenosine

#### General information

All solvents and reagents were supplied by Sigma Aldrich and were used as is unless explicitly stated, and phosphodexoxycytosine phosphoadenosine (pCA) was obtained through GE Healthcare/Dharmacon. Dry nitrogen was supplied by Praxair and passed through two moisture-scrubbing columns of dry calcium sulfate (Drierite) before use. HPLC analyses were performed on a Waters 1525 Binary HPLC pump equipped with a Waters 2998 Photodiode Array Detector by using Sunfire C18 analytical (3.5

$\mu\text{m}$ ,  $4.6 \times 150 \text{ mm}$ ,  $0.8 \text{ ml/min}$ ) or preparative ( $5.0 \mu\text{m}$ ,  $19 \times 150 \text{ mm}$ ,  $10 \text{ ml/min}$ ) columns and Empower software; buffers were drawn in linear gradients from 100% A (50 mM ammonium acetate) to 100% B (acetonitrile) over 30 min. UV-visible spectra for concentration determinations were recorded on a Thermo Fisher Scientific Nanodrop 2000C spectrophotometer. Mass spectra were recorded on a Waters Q ToF Premier Quadrupole instrument, in both positive and negative modes.

#### Cyanomethyl ester of Boc-L-citrulline

The cyanomethyl ester of Boc-L-citrulline was prepared and purified as described previously (Robertson et al., 1991).

#### Citrulline-pCA

Slight modifications from the published procedure were used (Robertson et al., 1991; Hohsaka et al., 1999). The cyanomethyl ester of Boc-L-citrulline (0.04 mmol) and pCA (5 mg, 0.008 mmol) were dissolved in dry dimethylformamide (200  $\mu\text{l}$ ) in a screw-top vial (1 dram) and tetrabutylammonium acetate (30 mg, 0.1 mmol) was added. The solution was stoppered and stirred at room temperature and monitored by HPLC over several hours (2- $\mu\text{l}$  aliquots were removed and diluted into 100  $\mu\text{l}$  of a 4:1 mixture of A/B buffer before injection) with detection at 261 nm. Unreacted pCA elutes at  $\sim 9$  min, and the Boc-L-citrulline pCA product elutes around 10–13 min. The reaction was judged complete after consumption of free pCA, after  $\sim 4$  h. The reaction was divided equally into  $8 \times 1.5\text{-ml}$  tubes, and  $\sim 1$  ml ice-cold ether was introduced to each, resulting in a cloudy precipitate, which was centrifuged down to a pellet (10,000 rpm, 1 min). The eight pellets were then each resuspended in 50  $\mu\text{l}$  acetonitrile and precipitated again with 1 ml ether. After a third round of precipitation, the eight tubes were combined into one and precipitated a fourth time, then dried in a gentle stream of dry nitrogen gas after centrifugation. Approximately 300  $\mu\text{l}$  ice-cold trifluoroacetic acid was added, and the pellet was dissolved via agitation and pipetting and placed on an ice bath for 30 min to remove the Boc group. Excess trifluoroacetic acid was removed in a gentle stream of dry nitrogen gas until a sticky oil remained, and ice-cold ether was added to precipitate the trifluoroacetic acid salt of L-Citrulline-pCA, which was washed twice more with ether and very carefully dried in a gentle stream of dry nitrogen gas. The resulting granular powder was stored as a salt at  $-20^\circ\text{C}$ . For ligation to -CA tRNA, this material was carefully dissolved in  $\sim 50 \mu\text{l}$  dry DMSO and checked for product integrity via HPLC, and stock concentration was approximated on a NanoDrop UV-vis spectrometer by using the known molecular extinction coefficient for pCA. L-Citrulline-pCA isolated in this manner had its concentration adjusted to 3 mM with DMSO, and the stock was stored in aliquots at  $-28^\circ\text{C}$ .

#### In vivo nonsense suppression in *X. laevis* oocytes

Mutations were made into the WT inactivation-removed ( $\Delta 6\text{--}46$ ) *Shaker* in the pBSTA vector by using standard methods. Complementary RNA (cRNA) was transcribed via the Ambion mMES SAGE mMACHINE T7 kit. Truncated pyrrolysine tRNA (lacking the last two nucleotides) was chemically synthesized and HPLC purified by Integrated DNA Technologies, Inc. Folding

was accomplished as follows: tRNA was resuspended in 10 mM HEPES and 3 mM  $\text{MgCl}_2$ , pH 7.5, and then moved to a thermocycler wherein a protocol was run with heating to  $94^\circ\text{C}$  for 3 min followed by linear cooling to  $4^\circ\text{C}$  over the course of 20 min. Ligation and recovery of the refolded tRNA was done as previously described in detail (Leisle et al., 2016). *X. laevis* oocytes were purchased from Ecocyte Inc. and co-injected with 25 ng cRNA bearing a TAG mutation at the site of encoding and  $\sim 150$  ng of pyrrolysine tRNA appended with either pCA-citrulline or the pCA alone as a negative control. For recording of WT *Shaker* and conventional mutations, 1–10 ng cRNA was injected. Recordings were made 20–30 h postinjection.

#### Electrophysiology

Two-electrode voltage-clamp (TEVC) recordings were made in standard Ringer's solution containing (in mM) 116 NaCl, 2 KCl, 1.8  $\text{CaCl}_2$ , 2  $\text{MgCl}_2$ , and 5 HEPES. The holding potential was  $-80$  mV. G-V values were derived from isochronal tail currents from cells expressing at least  $1 \mu\text{A}$  of tail current, for all variants except R368Q-*Shaker*, which closed too quickly to reliably quantify tail currents. In this case, we derived G-V values from ionic currents, assuming a reversal potential for potassium of  $-80$  mV. The data we derived from R368Q was in good agreement with those published previously. Cut-open voltage-clamp (COVC) recordings from oocytes expressing *Shaker* variants were done as described previously (Stefani and Bezanilla, 1998). Gpatch, an in-house program, controlled an SB6711 digital signal processor-based board sampling at 40  $\mu\text{s/point}$  (Innovative Integration) with an A4D4 board (Innovative Integration). Oocytes were held under voltage-clamp with a Dagan CA-1B amplifier, and current was filtered at 5 kHz. All recordings were performed around  $18^\circ\text{C}$ , with an external solution containing (in mM) 12 potassium methylsulfonate (MES), 10 HEPES, and 2  $\text{Ca}(\text{OH})_2$  and an internal solution containing (in mM) 120 K-MES, 10 HEPES, and 2 EGTA. Both solutions were set to pH 7.5. Microelectrodes were pulled on a Flaming/Brown micropipette puller (model P-87, Sutter Instruments), were filled with 3 M KCl, and had a resistance of  $\sim 0.2\text{--}0.8 \text{ M}\Omega$ . For both TEVC and COVC recordings, G-V values were fit to a two-state model.

#### Structural depictions

Models were made from PDB accession no. 2R9R by using Pymol.

#### Online supplemental material

Fig. S1 shows mass spectrometry confirming the identity of the Citrulline-pCA substrate before ligation to tRNA.

## Results

#### Encoding of citrulline in the voltage sensor of *Shaker*

Substitution of arginine with citrulline was achieved by nonsense suppression with chemically aminoacylated tRNA (Nowak et al., 1998). Coinjection of citrulline-acylated pyrrolysine tRNA (Pyl-citrulline) with cRNA of *Shaker* potassium channels with TAG stop codons at R362, R368, and R371 yielded robust voltage-activated potassium currents as measured by two-electrode voltage clamp. In Fig. 2 B, we have quantified the amount of ionic

current observed at +50 mV at each site, in comparison with the same cRNA co-injected with unacylated, full-length (pCA-ligated) pyrrolysine tRNA. Currents were not seen in the absence of appended amino acid, reflective of the orthogonality of this tRNA species in the *X. laevis* oocyte (Infield et al., 2018). Ionic currents were not observed from injection of citrulline-acylated tRNA with cRNA encoding R2TAG (R365) or R6TAG (R377), signifying either that these sites were not efficiently “rescued” by Pyl-citrulline or that citrulline incorporation rendered the channels nonfunctional. Although the charge at R6 has been previously implicated in channel trafficking, R2 is tolerant of side-chain mutagenesis (Papazian et al., 1991). The specific reasons for our lack of observed current at these positions is unclear and perhaps a subject for future studies. The expression levels achieved from rescue at R1, R3, and R4 compare favorably with previous studies encoding other polar unnatural amino acids into *Shaker* (Pless et al., 2011), enabling detailed characterization of macroscopic ionic currents but not the direct assessment of S4 movement via gating-current measurement. Therefore, the results reported here represent an indirect assessment of gating-charge function. It should be noted that gating currents have been recorded from *Shaker* channels wherein the unnatural amino acid ANAP was encoded via the evolved synthetase system, and thus the requisite expression levels are compatible with nonsense suppression per se (Kalstrup and Blunck, 2013).

#### Effects of citrulline substitution at R1 or R3 on *Shaker* activation

R1 (R362) is the outermost arginine in the S4 voltage sensor of *Shaker*. During activation, this arginine has been proposed to move outward from a location near the bottom of the hydrophobic plug to the extracellular environment. In *Shaker*, conventional mutation of R362 shifts the G-V in a depolarized direction, 30–40 mV. This is true whether the side chain is neutralized with glutamine (Papazian et al., 1991) or eliminated with alanine (Chowdhury et al., 2014). For the purpose of comparison, we also recorded R362Q-*Shaker* and indeed, we note an ~30 mV shift in the  $V_{1/2}$  for activation as compared with WT, and the activation slope was also decreased (Table 1). In contrast, when R362 was mutated to citrulline, the activation of the channels was similar to WT (Fig. 3 D):  $V_{1/2}$  of  $-19.4 \pm 3.5$  mV and  $-25 \pm 1.7$  mV for WT and R362Cit, respectively. Thus, the charge at position R1 is apparently expendable for channel function when side chain structure is not concomitantly altered.

R3 (R368) is proposed to traverse the electric field in response to depolarization; data from structural and molecular dynamics studies suggest that this amino acid is electrostatically bonded to E0 (E247) in the activated voltage sensor. Previous studies have demonstrated that mutation of R368 to either glutamine or alanine results in >70-mV shifts in the G-V to the right (Perozo et al., 1994; Chowdhury et al., 2014), but mutation to asparagine or methionine (Aggarwal and MacKinnon, 1996; Seoh et al., 1996) causes only minor effects. From these data, steric and electrostatic roles for arginine can be suggested but not well quantified. In our hands, the  $V_{1/2}$  for activation for the R368Q mutant was shifted ~100 mV to the right relative to WT *Shaker*, and the activation slope was significantly shallowed (Fig. 4 C and Table 1).

Table 1. Gating parameters for glutamine and citrulline substitution in the voltage sensor

	n	$V_{1/2}$	SD	Z	SD
WT	9	-19.4	3.5	2.8	0.7
WT (COVC)	3	-15.4	1.4	2.1	0.2
R362Q	5	12.0	3.0	1.5	0.1
R362CIT	6	-25.2	1.7	2.4	0.2
R368Q	5	79.8	3.9	1.3	0.1
R368CIT	6	-1.4	5.3	1.5	0.3
R371Q (COVC)	6	-29.7	3.6	2.7	0.7
R371CIT (COVC)	6	-56.7	1.7	3.1	0.5

When we instead encoded citrulline into this site, the  $V_{1/2}$  for activation was modestly affected with an ~18-mV shift rightward compared with WT *Shaker*. Interestingly, although there was a 78-mV difference in the activation midpoints between R3Cit and R3Q, the activation slope of R3Cit was shallowed to a similar degree as R3Q (Table 1). These data are indeed consistent with a net electrostatic effect of the R3 positive charge on voltage dependence of activation, although the effect attributable to charge is significantly milder than when shape is concomitantly altered. Thus, in addition to enabling a quantification of electrostatic contributions to channel function, the data from R1 and R3 highlight the extent to which changes in the shape of arginine at these positions cause strong deleterious effects within this voltage sensor.

#### Effect of encoding citrulline into R4

Within the S4 voltage sensor, R4 (R371 in *Shaker*) is the most cytoplasmic arginine to cross the hydrophobic plug during activation (Yang et al., 1996). Mutation of this residue to glutamine has been reported to generate a small hyperpolarizing left shift in G-V (Seoh et al., 1996), although elimination of the side chain via alanine substitution generates a larger leftward shift (Chowdhury et al., 2014). Interestingly, mutation of R371 to lysine causes a large (>60 mV) depolarizing rightward shift in G-V (Papazian et al., 1991). The large functional effect of this conservative mutation may be caused by an alteration in the interaction of this amino acid with the highly conserved F290 in the hydrophobic plug (Lacroix and Bezanilla, 2011). During initial TEVC recordings, we noted a large hyperpolarizing shift in the resting membrane potential of R371Cit-expressing cells ( $-76 \pm 5$  mV in R371Cit versus  $-41 \pm 5$  mV for WT *Shaker*), consistent with a standing potassium conductance. We therefore decided to record this and related variants using the cut-open voltage-clamp technique, which allows control of intracellular as well as extracellular ionic composition (Stefani and Bezanilla, 1998). By using this configuration, R371Q-*Shaker* demonstrated a left shift in  $V_{1/2}$  of ~14 mV (Fig. 5 D). In contrast, when citrulline was encoded, the G-V relationship was shifted significantly further to the left ( $-\Delta V_{1/2}$  of ~41 mV). Both activation and deactivation kinetics were affected by neutralization of R371 with Citrulline; activation was slowed three- to fourfold depending on the test voltage, and

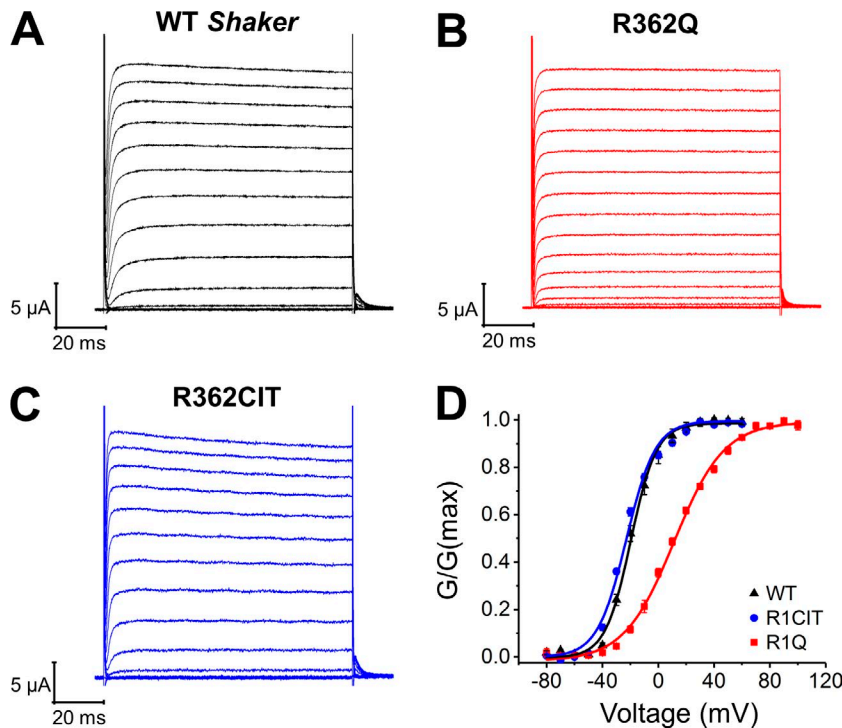


Figure 3. **Lack of effect on activation of encoding citrulline at R1 in *Shaker*.** (A–C) Voltage-dependent ionic currents from oocytes expressing WT, R362CIT-, and R362Q-*Shaker* channels. Oocytes were held at  $-80$  mV and subjected to 100-ms pulses in 10-mV steps, followed by 100-ms pulses to  $-50$  mV (WT, Cit) or  $-40$  mV (Q) before returning to the holding potential. (D) Normalized G-V values. Error bars represent  $\pm$ SEM. At R1, a positive charge is apparently dispensable for activation, provided the shape of arginine is maintained.

deactivation kinetics were profoundly slowed between 50- and 100-fold (Fig. 5, E and F).

## Discussion

Here we report the first examples of *in vivo* site-directed encoding of citrulline, a neutral analogue of the canonical amino acid arginine. We substituted the conserved arginine residues in the voltage sensor of *Shaker*, a model voltage-gated potassium channel. In the case of R1Cit and R3Cit, we noted modest defects compared with respective glutamine and alanine mutations (Chowdhury et al., 2014). These results support the idea that in the voltage-sensing domain, a crowded structural environment around S4 has evolved to accommodate the guanidinium moieties of the arginine residues, and that altering the precise lock-and-key nature of this fit results in defects in activation that are not completely related to changes in charge. The behavior of R1Cit was essentially identical

to WT *Shaker*, which leads us to conclude that a positive charge at R1 is dispensable for normal channel function. However, it is important to note that this interpretation does not exclude the possibility that R1 interacts with negatively charged amino acids during various resting, intermediate, or active conformations. Instead, the data indicate that any such interactions, in aggregate, do not have major effects on channel activation. It should also be noted that the slope of the G-V curve, as measured here, does not give the real charge contribution of R1 to the gating current because it has not been measured at low-enough open probability. Nonetheless, our data may provide one explanation as to why R1 is not universally conserved in potassium channel voltage-sensing domains. In contrast to R1, R3Cit was right shifted relative to WT *Shaker*, although not as substantially as with glutamine or alanine. This result is consistent with the notion that a positive charge at this position plays a role in activation in the native channel, as proposed in prior work (Tiwari-Woodruff et al., 2000).

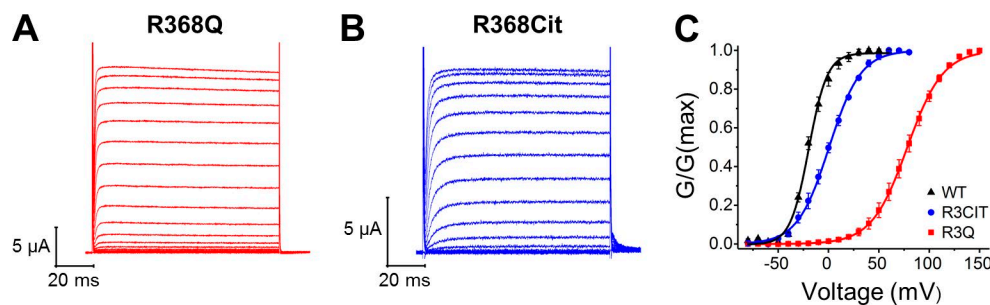


Figure 4. **Effects on activation of encoding citrulline at R3 in *Shaker*.** (A and B) Voltage-dependent ionic currents from oocytes expressing R368CIT- and R368Q-*Shaker* channels. Oocytes were held at  $-80$  mV and subjected to 100-ms pulses in 10-mV steps, followed by 100-ms pulses to  $-40$  mV (Cit) or  $-30$  mV (Q) before returning to the holding potential. (C) Normalized G-V values. Error bars represent  $\pm$ SEM. Note that the same WT data are used here and in Fig. 3 D. At R3, neutralization via citrulline resulted in a rightward shift and change in activation slope, suggesting that a positive charge at this position is necessary for normal activation. However, the effect on activation is modest compared with mutation to glutamine.

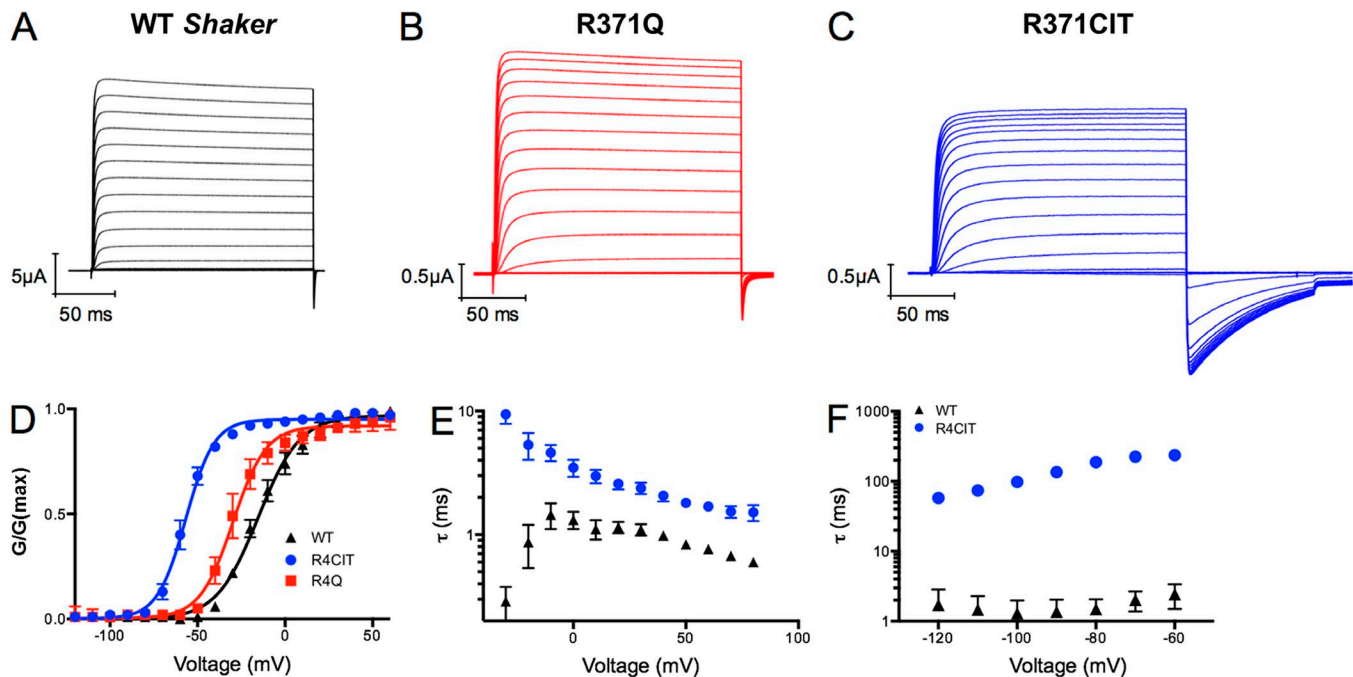


Figure 5. **Outsized electrostatic role for R4 in channel deactivation.** (A–C) Normalized G–V curves from COVC of WT-, R371Q-, and R371Cit-*Shaker*. Oocytes were held at  $-80$  mV, then prepulsed to  $-120$  mV for 200 ms, before a variable pulse ranging from  $80$  mV to  $-120$  mV, followed by a postpulse to  $-120$  mV, before returning to the original holding potential. (D) Normalized G–V values. Error bars represent  $\pm$ SEM. (E) A comparison of the activation rate ( $\tau$ ) between WT- and R371Cit-*Shaker* as derived from the same data used for the G–V curves. (F) Deactivation rate for WT- and R371Cit-*Shaker*. For these data, oocytes were held at  $-80$  mV, prepulsed to  $-120$  mV for 200 ms, then pulsed to  $80$  mV for 50 ms, followed by a variable pulse ranging from  $80$  mV to  $-120$  mV for 350 ms, before returning to the original holding potential.

The neutralization of R4 (R371) via citrulline strongly hyperpolarized the activation midpoint, and it slowed activation and drastically slowed deactivation kinetics. One mechanistic explanation for the energetic and kinetic effects of neutralization of R4 emerges from a consideration of the positioning of gating charges in the activated versus the deactivated states of the voltage sensor. Functional and computational experiments support the idea that the electric field across the voltage-sensing domain is narrowly focused over a region of  $<5$  Å (Asamoah et al., 2003; Ahern and Horn, 2005; Bond and Sansom, 2007; Callenberg et al., 2012), and it is centered on the hydrophobic plug containing F290 at its most intracellular portion. Transfer across this hydrophobic region is expected to be energetically unfavorable for large, polar amino acids such as arginine (Schwaiger et al., 2012). During activation, this energetic barrier is overcome by voltage directly acting on charged amino acids within the electric field. In the case of citrulline substitution at R4, the first three arginines are expected to cross quickly; however, with Cit in the fourth position, the shape and polarity of arginine is preserved, but the site would no longer be expected to sense voltage. Therefore, regardless of direction, movement through the hydrophobic plug would be expected to be slowed for R4Cit. Because the opening and closing of the gate occurs only when R4 moves (Lacroix and Bezanilla, 2011), the ionic conductances will be slowed down (Fig. 5, E and F), even though the other three charges may translocate normally. Spectroscopic, cross-linking, and structural studies indicate that R4 is intracellular to the electrical field in the hyperpolarized, inactive state of the voltage sensor (Pathak et al., 2007; Henrion et al., 2012; Guo et al., 2016). Conversely, in the active state, the position of R4 places

it within the electric field (Long et al., 2007); during deactivation, it may drive the downward movement of S4 in response to hyperpolarization. The effect of neutralization of R4 may thus be more prominent on deactivation than activation. The data are equally consistent with the possibility that specific electrostatic interactions with R4 (potentially in the resting state of the VSD) play a role in catalyzing S4 movement or that loss of charge at R4 may fundamentally alter its interaction with the hydrophobic plug and that, in either case, neutralization more profoundly affects deactivation compared with activation.

In this study, citrulline was used as an analogue to quantify the effects of loss of positive charge on voltage-sensing arginine residues in a voltage-gated potassium channel. In recent years, citrullination (the posttranslational deimination of arginine residues) has been detected in an ever-increasing number of targets (Witalison et al., 2015). Research in this area is currently focused on extracellular targets wherein citrullination causes autoimmune diseases (Schellekens et al., 1998; van Venrooij and Pruijn, 2000) and on the role of citrullination of arginine residues in controlling gene transcription (Cuthbert et al., 2004; Wang et al., 2004). Thus far, mass spectroscopy identification of intracellular targets has focused on small soluble proteins; thus, there is a paucity of identified citrullinated sites within integral membrane proteins. However, VDACC1, a voltage-dependent and weakly anion-selective channel, has been shown to be citrullinated in disease states in both the brain and the heart (Jang et al., 2008; Fert-Bober et al., 2015). As the citrulline proteome continues to expand and more integral membrane proteins are identified, the ability to encode citrulline in vivo in a site-specific manner may

prove a valuable tool to understand the functional effects of this posttranslational modification.

## Acknowledgments

We thank Kin Lam and Dr. Emad Tajkhorshid (Department of Physics, Department of Biochemistry, Center for Biophysics and Quantitative Biology, National Institutes of Health Center for Macromolecular Modeling and Bioinformatics, Beckman Institute for Advanced Science and Technology, University of Illinois at Urbana-Champaign, Urbana, IL) for generating the electrostatic potential surface maps shown in Fig. 2.

This work was supported by National Institutes of Health grants R01GM106569 and R24NS104617 to C.A. Ahern and R01GM030376 to F. Bezanilla and Cystic Fibrosis Foundation grant INFIELD17F0 to D.T. Infield.

The authors declare no competing financial interests.

Author contributions: D.T. Infield, C.A. Ahern, and F. Bezanilla designed research. D.T. Infield, E.E.L. Lee, J.D. Galpin, and G.D. Galles performed research. D.T. Infield and E.E.L. Lee analyzed data. D.T. Infield wrote the manuscript. All authors edited and approved the final version of the manuscript.

Kenton J. Swartz served as editor.

Submitted: 28 March 2018

Accepted: 8 May 2018

## References

- Aggarwal, S.K., and R. MacKinnon. 1996. Contribution of the S4 segment to gating charge in the Shaker K<sup>+</sup> channel. *Neuron*. 16:1169–1177. [https://doi.org/10.1016/S0896-6273\(00\)80143-9](https://doi.org/10.1016/S0896-6273(00)80143-9)
- Ahern, C.A., and R. Horn. 2005. Focused electric field across the voltage sensor of potassium channels. *Neuron*. 48:25–29. <https://doi.org/10.1016/j.neuron.2005.08.020>
- Ahuja, S., S. Mukund, L. Deng, K. Khakh, E. Chang, H. Ho, S. Shriver, C. Young, S. Lin, J.P. Johnson Jr., et al. 2015. Structural basis of Nav1.7 inhibition by an isoform-selective small-molecule antagonist. *Science*. 350:aac5464. <https://doi.org/10.1126/science.aac5464>
- Asamoah, O.K., J.P. Wuskell, L.M. Loew, and F. Bezanilla. 2003. A fluorometric approach to local electric field measurements in a voltage-gated ion channel. *Neuron*. 37:85–98. [https://doi.org/10.1016/S0896-6273\(02\)01126-1](https://doi.org/10.1016/S0896-6273(02)01126-1)
- Bezanilla, F. 2000. The voltage sensor in voltage-dependent ion channels. *Physiol. Rev.* 80:555–592. <https://doi.org/10.1152/physrev.2000.80.2.555>
- Bezanilla, F., and E. Perozo. 2003. The voltage sensor and the gate in ion channels. *Adv. Protein Chem.* 63:211–241. [https://doi.org/10.1016/S0065-3233\(03\)63009-3](https://doi.org/10.1016/S0065-3233(03)63009-3)
- Bond, P.J., and M.S. Sansom. 2007. Bilayer deformation by the Kv channel voltage sensor domain revealed by self-assembly simulations. *Proc. Natl. Acad. Sci. USA*. 104:2631–2636. <https://doi.org/10.1073/pnas.0606822104>
- Burschowsky, D., A. van Eerde, M. Ökvist, A. Kienhöfer, P. Kast, D. Hilvert, and U. Krengel. 2014. Electrostatic transition state stabilization rather than reactant destabilization provides the chemical basis for efficient chorismate mutase catalysis. *Proc. Natl. Acad. Sci. USA*. 111:17516–17521. <https://doi.org/10.1073/pnas.1408512111>
- Callenberg, K.M., N.R. Latorraca, and M. Grabe. 2012. Membrane bending is critical for the stability of voltage sensor segments in the membrane. *J. Gen. Physiol.* 140:55–68. <https://doi.org/10.1085/jgp.201110766>
- Cannon, S.C. 2010. Voltage-sensor mutations in channelopathies of skeletal muscle. *J. Physiol.* 588:1887–1895. <https://doi.org/10.1113/jphysiol.2010.186874>
- Choudhury, A.K., S.Y. Golovine, L.M. Dedkova, and S.M. Hecht. 2007. Synthesis of proteins containing modified arginine residues. *Biochemistry*. 46:4066–4076. <https://doi.org/10.1021/bi062042r>
- Chowdhury, S., B.W. Jarecki, and B. Chanda. 2014. A molecular framework for temperature-dependent gating of ion channels. *Cell*. 158:1148–1158. <https://doi.org/10.1016/j.cell.2014.07.026>
- Cuthbert, G.L., S. Daujat, A.W. Snowden, H. Erdjument-Bromage, T. Hagiwara, M. Yamada, R. Schneider, P.D. Gregory, P. Tempst, A.J. Bannister, and T. Kouzarides. 2004. Histone deimination antagonizes arginine methylation. *Cell*. 118:545–553. <https://doi.org/10.1016/j.cell.2004.08.020>
- Delemotte, L., M.A. Kasimova, M.L. Klein, M. Tarek, and V. Carnevale. 2015. Free-energy landscape of ion-channel voltage-sensor-domain activation. *Proc. Natl. Acad. Sci. USA*. 112:124–129. <https://doi.org/10.1073/pnas.1416959112>
- Fert-Bober, J., J.T. Giles, R.J. Holewinski, J.A. Kirk, H. Uhrigshardt, E.L. Crowley, F. Andrade, C.O. Bingham III, J.K. Park, M.K. Halushka, et al. 2015. Citrullination of myofibrillar proteins in heart failure. *Cardiovasc. Res.* 108:232–242. <https://doi.org/10.1093/cvr/cvv185>
- Gamble, J.G., and A.L. Lehninger. 1973. Transport of ornithine and citrulline across the mitochondrial membrane. *J. Biol. Chem.* 248:610–618.
- Guo, J., W. Zeng, Q. Chen, C. Lee, L. Chen, Y. Yang, C. Cang, D. Ren, and Y. Jiang. 2016. Structure of the voltage-gated two-pore channel TPC1 from *Arabidopsis thaliana*. *Nature*. 531:196–201. <https://doi.org/10.1038/nature16446>
- György, B., E. Tóth, E. Tarcsa, A. Falus, and E.I. Buzás. 2006. Citrullination: A posttranslational modification in health and disease. *Int. J. Biochem. Cell Biol.* 38:1662–1677. <https://doi.org/10.1016/j.biocel.2006.03.008>
- Henrion, U., J. Renhorn, S.I. Börjesson, E.M. Nelson, C.S. Schwaiger, P. Bjelkmar, B. Wallner, E. Lindahl, and F. Elinder. 2012. Tracking a complete voltage-sensor cycle with metal-ion bridges. *Proc. Natl. Acad. Sci. USA*. 109:8552–8557. <https://doi.org/10.1073/pnas.1116938109>
- Hohsaka, T., D. Kajihara, Y. Ashizuka, and H. Murakami. 1999. Efficient incorporation of nonnatural amino acids with large aromatic groups into streptavidin in vitro protein synthesizing systems. *J. Am. Chem. Soc.* 121:34–40. <https://doi.org/10.1021/ja9813109>
- Infield, D.T., J.D. Lueck, J.D. Galpin, G.D. Galles, and C.A. Ahern. 2018. Orthogonality of pyrrolysine tRNA in the *Xenopus* oocyte. *Sci. Rep.* 8:5166. <https://doi.org/10.1038/s41598-018-23201-z>
- Jan, L.Y., and Y.N. Jan. 2012. Voltage-gated potassium channels and the diversity of electrical signalling. *J. Physiol.* 590:2591–2599. <https://doi.org/10.1113/jphysiol.2011.224212>
- Jang, B., E. Kim, J.K. Choi, J.K. Jin, J.I. Kim, A. Ishigami, N. Maruyama, R.I. Carp, Y.S. Kim, and E.K. Choi. 2008. Accumulation of citrullinated proteins by up-regulated peptidylarginine deiminase 2 in brains of scrapie-infected mice: A possible role in pathogenesis. *Am. J. Pathol.* 173:1129–1142. <https://doi.org/10.2353/ajpath.2008.080388>
- Jensen, M.O., V. Jogini, D.W. Borhani, A.E. Leffler, R.O. Dror, and D.E. Shaw. 2012. Mechanism of voltage gating in potassium channels. *Science*. 336:229–233. <https://doi.org/10.1126/science.1216533>
- Judice, J.K., T.R. Gamble, E.C. Murphy, A.M. de Vos, and P.G. Schultz. 1993. Probing the mechanism of staphylococcal nuclease with unnatural amino acids: kinetic and structural studies. *Science*. 261:1578–1581. <https://doi.org/10.1126/science.8103944>
- Kalstrup, T., and R. Blunck. 2013. Dynamics of internal pore opening in K(V) channels probed by a fluorescent unnatural amino acid. *Proc. Natl. Acad. Sci. USA*. 110:8272–8277. <https://doi.org/10.1073/pnas.1220398110>
- Kienhöfer, A., P. Kast, and D. Hilvert. 2003. Selective stabilization of the chorismate mutase transition state by a positively charged hydrogen bond donor. *J. Am. Chem. Soc.* 125:3206–3207. <https://doi.org/10.1021/ja0341992>
- Lacroix, J.J., and F. Bezanilla. 2011. Control of a final gating charge transition by a hydrophobic residue in the S2 segment of a K<sup>+</sup> channel voltage sensor. *Proc. Natl. Acad. Sci. USA*. 108:6444–6449. <https://doi.org/10.1073/pnas.1103397108>
- Leisle, L., R. Chadda, J.D. Lueck, D.T. Infield, J.D. Galpin, V. Krishnamani, J.L. Robertson, and C.A. Ahern. 2016. Cellular encoding of Cy dyes for single-molecule imaging. *eLife*. 5:e19088. <https://doi.org/10.7554/eLife.19088>
- Long, S.B., E.B. Campbell, and R. MacKinnon. 2005. Voltage sensor of Kv1.2: Structural basis of electromechanical coupling. *Science*. 309:903–908. <https://doi.org/10.1126/science.1116270>
- Long, S.B., X. Tao, E.B. Campbell, and R. MacKinnon. 2007. Atomic structure of a voltage-dependent K<sup>+</sup> channel in a lipid membrane-like environment. *Nature*. 450:376–382. <https://doi.org/10.1038/nature06265>
- Nakata, M., T. Yada, S. Nakagawa, K. Kobayashi, and I. Maruyama. 1997. Citrulline-argininosuccinate-arginine cycle coupled to Ca<sup>2+</sup>-signaling

- in rat pancreatic beta-cells. *Biochem. Biophys. Res. Commun.* 235:619–624. <https://doi.org/10.1006/bbrc.1997.6854>
- Nowak, M.W., J.P. Gallivan, S.K. Silverman, C.G. Labarca, D.A. Dougherty, and H.A. Lester. 1998. In vivo incorporation of unnatural amino acids into ion channels in *Xenopus* oocyte expression system. *Methods Enzymol.* 293:504–529. [https://doi.org/10.1016/S0076-6879\(98\)93031-2](https://doi.org/10.1016/S0076-6879(98)93031-2)
- Ottosson, N.E., S.I. Liin, and F. Elinder. 2014. Drug-induced ion channel opening tuned by the voltage sensor charge profile. *J. Gen. Physiol.* 143:173–182. <https://doi.org/10.1085/jgp.201311087>
- Papazian, D.M., L.C. Timpe, Y.N. Jan, and L.Y. Jan. 1991. Alteration of voltage-dependence of Shaker potassium channel by mutations in the S4 sequence. *Nature.* 349:305–310. <https://doi.org/10.1038/349305a0>
- Pathak, M.M., V. Yarov-Yarovoy, G. Agarwal, B. Roux, P. Barth, S. Kohout, F. Tombola, and E.Y. Isacoff. 2007. Closing in on the resting state of the Shaker K(+) channel. *Neuron.* 56:124–140. <https://doi.org/10.1016/j.neuron.2007.09.023>
- Perozo, E., L. Santacruz-Tolozza, E. Stefani, F. Bezanilla, and D.M. Papazian. 1994. S4 mutations alter gating currents of Shaker K channels. *Biophys. J.* 66:345–354. [https://doi.org/10.1016/S0006-3495\(94\)80783-0](https://doi.org/10.1016/S0006-3495(94)80783-0)
- Pless, S.A., J.D. Galpin, A.P. Niciforovic, and C.A. Ahern. 2011. Contributions of counter-charge in a potassium channel voltage-sensor domain. *Nat. Chem. Biol.* 7:617–623. <https://doi.org/10.1038/nchembio.622>
- Robertson, S.A., J.A. Ellman, and P.G. Schultz. 1991. A general and efficient route for chemical aminocyclization of transfer RNAs. *J. Am. Chem. Soc.* 113:2722–2729. <https://doi.org/10.1021/ja00007a055>
- Schellekens, G.A., B.A. de Jong, F.H. van den Hoogen, L.B. van de Putte, and W.J. van Venrooij. 1998. Citrulline is an essential constituent of antigenic determinants recognized by rheumatoid arthritis-specific autoantibodies. *J. Clin. Invest.* 101:273–281. <https://doi.org/10.1172/JCI1316>
- Schwaiger, C.S., S.I. Börjesson, B. Hess, B. Wallner, F. Elinder, and E. Lindahl. 2012. The free energy barrier for arginine gating charge translation is altered by mutations in the voltage sensor domain. *PLoS One.* 7:e45880. <https://doi.org/10.1371/journal.pone.0045880>
- Seoh, S.A., D. Sigg, D.M. Papazian, and F. Bezanilla. 1996. Voltage-sensing residues in the S2 and S4 segments of the Shaker K+ channel. *Neuron.* 16:1159–1167. [https://doi.org/10.1016/S0896-6273\(00\)80142-7](https://doi.org/10.1016/S0896-6273(00)80142-7)
- Sokolov, S., T. Scheuer, and W.A. Catterall. 2007. Gating pore current in an inherited ion channelopathy. *Nature.* 446:76–78. <https://doi.org/10.1038/nature05598>
- Starace, D.M., and F. Bezanilla. 2001. Histidine scanning mutagenesis of basic residues of the S4 segment of the Shaker K+ channel. *J. Gen. Physiol.* 117:469–490. <https://doi.org/10.1085/jgp.117.5.469>
- Starace, D.M., E. Stefani, and F. Bezanilla. 1997. Voltage-dependent proton transport by the voltage sensor of the Shaker K+ channel. *Neuron.* 19:1319–1327. [https://doi.org/10.1016/S0896-6273\(00\)80422-5](https://doi.org/10.1016/S0896-6273(00)80422-5)
- Stefani, E., and F. Bezanilla. 1998. Cut-open oocyte voltage-clamp technique. *Methods Enzymol.* 293:300–318. [https://doi.org/10.1016/S0076-6879\(98\)93020-8](https://doi.org/10.1016/S0076-6879(98)93020-8)
- Tao, X., A. Lee, W. Limapichat, D.A. Dougherty, and R. MacKinnon. 2010. A gating charge transfer center in voltage sensors. *Science.* 328:67–73. <https://doi.org/10.1126/science.1185954>
- Tiwari-Woodruff, S.K., M.A. Lin, C.T. Schulteis, and D.M. Papazian. 2000. Voltage-dependent structural interactions in the Shaker K+ channel. *J. Gen. Physiol.* 115:123–138. <https://doi.org/10.1085/jgp.115.2.123>
- Tombola, F., M.M. Pathak, and E.Y. Isacoff. 2005. Voltage-sensing arginines in a potassium channel permeate and occlude cation-selective pores. *Neuron.* 45:379–388. <https://doi.org/10.1016/j.neuron.2004.12.047>
- van Venrooij, W.J., and G.J. Pruijn. 2000. Citrullination: A small change for a protein with great consequences for rheumatoid arthritis. *Arthritis Res.* 2:249–251. <https://doi.org/10.1186/ar95>
- Wang, Y., J. Wysocka, J. Sayegh, Y.H. Lee, J.R. Perlin, L. Leonelli, L.S. Sonbuchner, C.H. McDonald, R.G. Cook, Y. Dou, et al. 2004. Human PAD4 regulates histone arginine methylation levels via demethylation. *Science.* 306:279–283. <https://doi.org/10.1126/science.1101400>
- Witalison, E.E., P.R. Thompson, and L.J. Hofseth. 2015. Protein arginine deiminases and associated citrullination: Physiological functions and diseases associated with dysregulation. *Curr. Drug Targets.* 16:700–710. <https://doi.org/10.2174/1389450116666150202160954>
- Yang, N., and R. Horn. 1995. Evidence for voltage-dependent S4 movement in sodium channels. *Neuron.* 15:213–218. [https://doi.org/10.1016/0896-6273\(95\)90078-0](https://doi.org/10.1016/0896-6273(95)90078-0)
- Yang, N., A.L. George Jr., and R. Horn. 1996. Molecular basis of charge movement in voltage-gated sodium channels. *Neuron.* 16:113–122. [https://doi.org/10.1016/S0896-6273\(00\)80028-8](https://doi.org/10.1016/S0896-6273(00)80028-8)
- Yellen, G. 1998. The moving parts of voltage-gated ion channels. *Q. Rev. Biophys.* 31:239–295. <https://doi.org/10.1017/S0033583598003448>